PMD Compensator and PMD Emulator

by Yu Mimura[*], Kazuhiro Ikeda[*], Tatsuya Hatano[*], Takeshi Takagi[*], Sugio Wako[*] and Hiroshi Matsuura[*]

ABSTRACT As a technology for increasing the capacity to meet the growing demand for communications in recent years, dense wavelength-division multiplexing (DWDM) is being implemented in tandem with achieving higher transmission rates on each channel. At next-generation transmission rates of 40 Gbps, it is expected that polarization mode dispersion (PMD) will be the main factor in the deterioration of transmission characteristics. Both first-order PMD and higher-order PMD can affect the performance of a high-speed optical transmission system. A PMD emulator capable of generating PMD up to the second-order is useful in estimating the performance degradation due to PMD and in optimizing the devices that compensate for this type of degradation. The present work is a programmable device based on variable Faraday rotators (VFRs) that is capable of emulating first-order and two components of second-order PMD. Various PMD conditions can be generated by the emulator and the measured values agree with theoretical simulations. Further, we propose a much simpler configuration for the PMD compensator (PMDC) with higher-order PMD canceller (HOPC), unifying the monitor sections of the PMDC and HOPC into one power monitor. Test results for our configuration in a 10-Gbps evaluation system are also reported.

1. INTRODUCTION

In response to the need for larger capacities in long-haul optical digital transmission, greater channel density has been achieved by wavelength division multiplexing (WDM), and the bit rate for each channel is also being increased.

At 40 Gbps, which is in the next generation of transmission rates, polarization mode dispersion (PMD), which does not present a problem at bit rates of 10 Gbps and below, can impose significant limitations on the distance over which transmission is possible [1]. Further, at the distances served by 10-Gbps transmission, which is currently becoming the mainstream technology, there are concerns that using fibers installed in previous years may, depending on the amount of PMD, cause problems in terms of system configuration [2].

In recent years there have been many programs to study PMD compensation (PMDC) [1), 3), 4)]. PMD arises from random birefringence, induced either by increasing the core eccentricity of single-mode fibers or by internal stress due to changes in lateral pressure or temperature. This gives rise to a phenomenon known as differential group delay (DGD), in which two orthogonal polarization modes, which should, in theory, be degenerating in fact diverge. In these programs, the PMDC may be controlled either as the DGD element in the PMDC, completely compensating for DGD in the transmission line, or, as the input state of polarization (SOP) aligned to the principal state of polarization (PSP) [2]. However, both of these compensation methods were only for DGD, which is first-order PMD.

PMD also contains higher-order components, and second-order PMD (SOPMD) impairment to pulse propagation and the system penalty cannot be neglected [2), 5)]. A PMD emulator, which is capable of generating a desired and stable PMD up to the second order, is useful in estimating the performance degradation due to PMD up to the second order and to optimize the devices compensating for this type of degradation. Up to now, several techniques have been proposed to emulate PMD by the use of polarization rotators in combination with polarization maintaining fibers (PMF) or birefringent crystals [6), 7)]. However, these techniques have difficulties controlling second-order PMD because of the frequency dependence of these effects. The present work relates to a programmable device capable of emulating first-order PMD and two components of second-order PMD based on a variable Faraday rotator (VFR). Various PMD conditions can be generated by the emulator and the measured values agree with theoretical simulations.

Further, compensating for second-order PMD completely requires a complicated configuration, such

[*] Transmissions & Components Dept., FITEL-Photonics Lab.

as a PMD emulator consisting of many DGD sections. Such a configuration can be expensive, and control speed becomes a problem. On the other hand, PMDC with a higher-order PMD canceller (HOPC) [8] is one type of PMDC, which, while unable to provide complete compensation for second-order PMD, has a simple configuration. The HOPC is only a polarizer that functions as a suppresser of PMD depolarization, with a polarization controller for SOP alignment to the transmissive axis of the polarizer. Therefore, a combination of conventional first-order PMDC with HOPC includes second-order PMD mitigation and is simple in configuration.

In this paper, we propose a much simpler configuration for a first-order PMDC with HOPC, unifying the feedback monitors for the PMDC and for the HOPC into one power monitor. Test results for our configuration in a 10-Gbps evaluation system are also reported.

2. SECOND-ORDER PMD

First- and second-order PMD vectors may be represented by

$$\vec{\tau} = \tau \cdot \vec{q} \quad (1)$$

$$\vec{\tau}_\omega = \tau_\omega \cdot \vec{q} + \tau \cdot \vec{q}_\omega \quad (2)$$

where: the subscript indicates differentiation, ω is the optical angular frequency, τ is the DGD, and $\vec{q}$ is the unit Stokes vector aligned with the PSP.

The absolute value of the second-order PMD vector is the SOPMD, the first term of the right side is a polarization-dependent chromatic dispersion (PCD) component which is parallel to the first-order PMD vector, and the second term of the right side is a polarization state depolarization (PSD) component which is perpendicular to the first-order PMD vector. The units for SOPMD, PCD, and PSD are ps^2, ps/nm, and ps respectively, but in this paper all are shown in units of ps^2 for simplicity.

For a PMD emulator that uses a concatenation of birefringent elements such as polarization maintaining fiber (PMF) or birefringent crystal, the PMD vector can be calculated recursively [7]. For the device consisting of m sections, first- and second-order PMD may be represented by

$$\tau = \sum_{n=1}^{m} R(m, n+1)\vec{\tau}_n \quad (3)$$

$$\tau_\omega = \sum_{n=1}^{m} R(m, n+1)(\vec{\tau}_{n\omega} + \vec{\tau}_n \times \vec{\tau}(n)) \quad (4)$$

where: $\vec{\tau}_n$ is the first-order PMD vector output by n-th DGD section, $\vec{\tau}(n)$ is the first-order PMD vector output by first n DGD sections, and R is defined with rotation matrix for the n-th DGD section (R_n), such that

$$\begin{aligned} &R(m, n) = R_m R_{m-1} \cdots R_n (m>n) \\ &R(m, m) = R_m \\ &R(m, m+1) = identity\ matrix \end{aligned} \quad (5)$$

Specifically, the DGD and SOPMD generated by two DGD sections may be represented as

$$\tau = \sqrt{\tau_1^2 + \tau_2^2 + 2\tau_1\tau_2 \cos 2} \quad (6)$$

$$\tau_\omega = \tau_1\tau_2 \sin 2\theta \quad (7)$$

where: τ_1 and τ_2 are the DGD of the two DGD sections, and θ is the rotational connection angle. The DGD and SOPMD are independent of frequency. In this case, because the SOPMD vector is always perpendicular to the first-order PMD vector, SOPMD has only the PSD component.

In contrast, the DGD and SOPMD generated by the concatenation of more than two DGD sections, have a periodic characteristic with respect to frequency, and the SOPMD has two components. The free spectrum range (FSR) of a device is determined by the length of each DGD section.

3. SECOND-ORDER PMD EMULATOR

3.1 Configuration

The PMD emulator consists of four DGD sections concatenated by three VFRs, which function as polarization rotators [9]. Figure 1 shows a schematic of the device, which can generate first- and second-order PMD. In order to achieve a single FSR, all DGD sections have the same DGD value of 7.5 ps. The resulting FSR is 133.3 GHz, and all phases of all DGD sections are tuned to it. In order to shift the DGD and SOPMD spectra in frequency while keeping the spectral profile constant, a common frequency shift has to be applied to all FSRs. This can be achieved by a phase shifter, or by temperature control of the DGD sections. Although the number of DGD sections in the PMD emulator constructed here is four, that number can be reduced by setting VFR angles to zero. For example, setting any two angles to zero reduces the number of DGD sections to two.

Because there is a natural correlation among DGD, PCD, PSD and SOPMD, these variables cannot be individually set to any arbitrary value. However, by the simultaneous non-linear fitting of more than one target profile, the rotational connection angles can be calculated. In the emulator constructed here the rotational connection angles of the VFRs can be set to the angles determined by fitting, and the error of the rotational connection

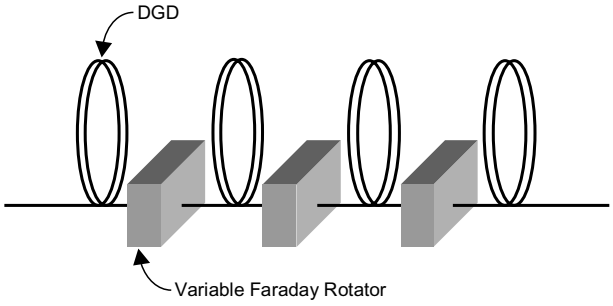

Figure 1 Schematic for the first- and second-order PMD emulator with VFRs.

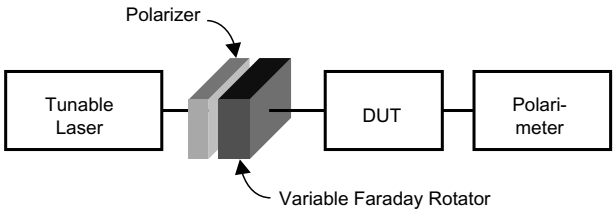

Figure 2 Schematic for the first- and second-order PMD measurement system with VFR.

angle with respect to the calculated value is less than ±3 degree.

The tunable DGD range of the PMD emulator is 0 to 30 ps, variable SOPMD range is 0 to 260 ps^2, and insertion loss of the device is 1.7 dB.

3.2 PMD Measurement System

Figure 2 shows the configuration of the PMD measurement system, which is based on the general polarization analysis method. The VFR is used as a polarization controller following a polarizer, which controls input SOP. A polarimeter is used as a Stokes analyzer, which analyzes output SOP. The PMD vector is analyzed by the Muller matrix method (MMM) [10], and is determined by measuring the two output Stokes vectors resulting from two orthogonal input Stokes vectors, and the first- and second-order PMD values and the components of SOPMD are calculated.

Two Stokes vector measurements performed at different wavelengths are required to determine the PMD vector at one wavelength. Because the SOPMD vector is the derivative of the PMD vector, determining the SOPMD vector at one wavelength requires Stokes vector measurement at one more wavelength. Determining SOPMD requires the measurement of at least two Stokes responses at three wavelengths. For an accurate determination, these measurements have to be completed before the PMD, the SOPMD and the polarization states of the DUT change. Utilizing a VFR that has a short response time for input SOP control, measurement time can be shortened and it is possible for measurement not to be affected by changes in the polarization state, which causes measurement error. Precision measurement of PMD and SOPMD can be effected by this system. The response time of the VFR for a $\pi/2$ rotation is less than 60 ms.

3.3 Results of Evaluation

With a fixed DGD spectrum, the SOPMD spectrum was changed by different values. The target DGD value was 20 ps at 1548 nm, and the target SOPMD values were 75, 100, and 125 ps^2. For each of the cases, a set of angles for the VFRs was calculated by simultaneous non-linear fitting:

SOPMD 75 ps^2 : 31.0, 67.5, 31.0 [deg.]
SOPMD 100 ps^2 : 26.4, 65.2, 26.4 [deg.]
SOPMD 125 ps^2 : 21.8, 63.5, 21.8 [deg.]

Figure 3 shows DGD and SOPMD by emulator and theory, and the two sets of values are consistent. Each measurement was carried out five times, and the data proved to be repeatable. Figure 4 shows the absolute values of PCD and PSD separated from SOPMD when the target SOPMD was set to 100 ps^2, demonstrating good agreement between the measured and theoretical values. Because PCD is zero at the center frequency, SOPMD includes only the PSD component at that frequency. The ratio of PCD to PSD increases as the

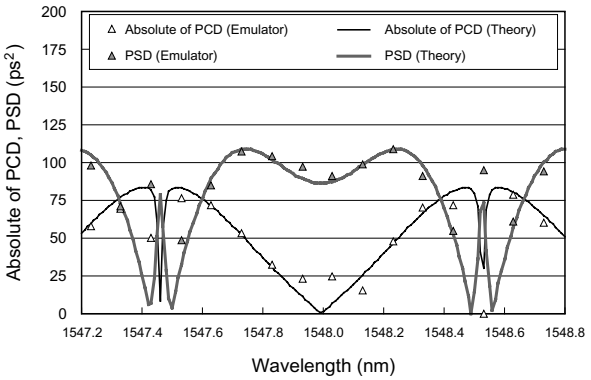

Figure 4 Absolute values of PCD and PSD separated from an SOPMD value of 100 ps^2.

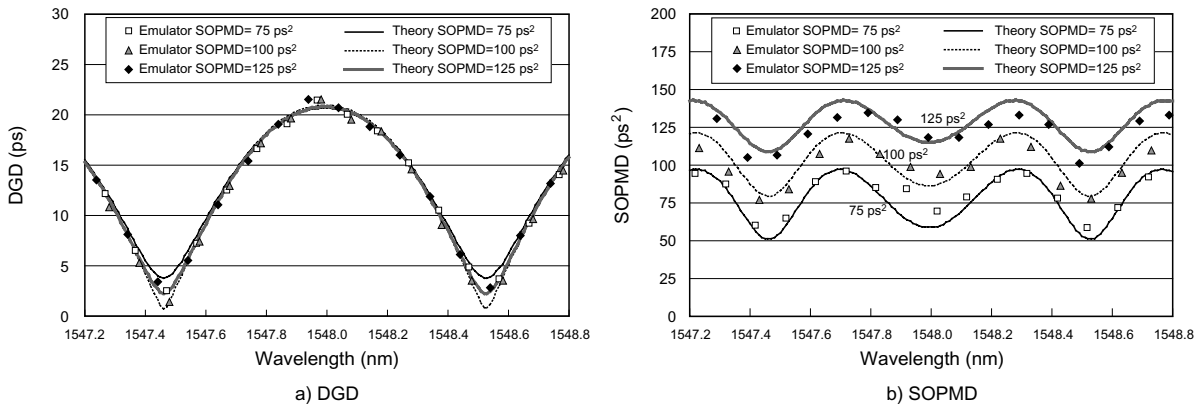

a) DGD b) SOPMD

Figure 3 DGD and SOPMD for SOPMD values of 75, 100 and 125 ps^2 by emulator and theory.

frequency deviates from the center frequency.

We also found that when the same frequency shift was applied to all FSRs, the DGD and SOPMD spectra shifted in frequency but kept the spectral profile. That is, the ratio of PCD to PSD at any one wavelength can be changed keeping SOPMD constant by shifting the spectra. This enables us to investigate the influence of two components of SOPMD on the transmission system.

The two-section configuration of the emulator can generate flat PMD spectrum in frequency. As mentioned above, setting any two angles to zero reduces the number of DGD sections to two. For example, when the angle of the first and third VFRs are set to zero, a two-section configuration of 15 ps + 15 ps is realized, and when the angles of the first and second VFRs are set to zero, a two-section configuration of 22.5 ps + 7.5 ps is realized. If the angle of the first VFR is set to 90 deg, the first and second DGD sections cancel each other, so the two-section configuration of 7.5 ps + 7.5 ps is realized with the last two DGD sections.

The two-section configuration of the emulator was also investigated. As in the four-section configuration test, target SOPMD was set to 75, 100, and 125 ps^2. Consistent with the theory, the measured SOPMD, DGD, PCD, and PSD were constant (not shown).

The above two tests demonstrate that, for a fixed SOPMD value, different PCD and PSD profiles can be achieved by changing the number of DGD sections in the emulator. The emulator's repeatability and programmability are useful for systematic testing and for the study of the real-time behavior of higher-order PMD.

4. SECOND-ORDER PMD COMPENSTOR

4.1 Configuration

In the conventional PMDC with HOPC shown in Figure 5 a) the compensator was configured with a PMDC [4] and an additional HOPC, which are completely independent of each other, while our novel PMDC with HOPC is shown in Figure 5 b) [8), 11)]. The first polarization controller and the PMF compose the first-order PMDC and the second polarization controller and a polarization beam splitter (PBS) compose the HOPC. The differences between our configuration and the conventional one are in the monitoring and control method. We use the other output port (not the signal port) of PBS to control both the first-order PMDC section and HOPC section.

In the conventional PMDC with HOPC shown in Figure 5 a), the degree of polarization (DOP) is monitored for control of the polarization controller of the PMDC, and output power from the polarizer is monitored for control of the polarization controller of the HOPC. Thus each polarization controller maximizes DOP and power individually, but if the polarization controller of the HOPC always maximizes power, maximizing DOP means the same as maximizing power, because DOP means polarization uniformity over the signal spectrum. If the polarization controller of the PMDC maximizes the power

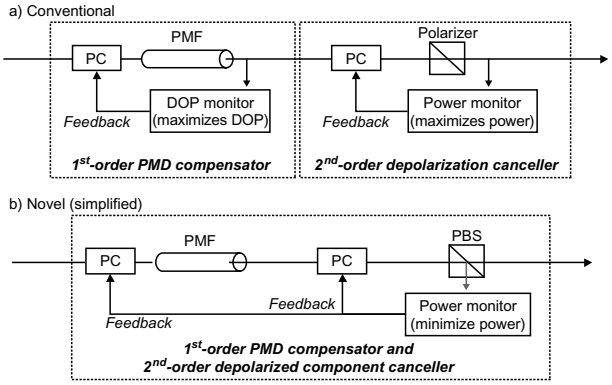

Figure 5 Configurations of conventional and novel PDMCs.

that is maximized by the polarization controller of the HOPC, it means that the DOP of the signal is maximized.

Therefore, we can unify DOP monitoring and power monitoring. Additionally, we monitor the other port of the PBS to reduce the number of components, and control the two polarization controllers so that the monitored power is minimized. This has the same meaning as maximizing the power from the signal port of the PBS. Thus, second-order PMD mitigation can be realized with a simplified configuration b) just as with configuration a).

4.2 Second-Order PMD Mitigation

It has been reported that the penalty due to second-order PMD is mainly caused by PSD components [2), 5)], so here we consider only PSD components. Theoretically, in a case in which the PSP is linearly polarized and aligned to x-axis and the direction of PSD depolarization is aligned to the direction while maintaining linear polarization, the output pulse which undergoes second-order PMD can be represented by the equation [2)].

$$\begin{aligned} \mathrm{E}_{out}(\eta) = \frac{K}{\sqrt{2}}\{&2\phi_+(\eta-\tau)(\hat{u}^*+\hat{u}) \\ &+[\Delta\phi_+(\eta-\tau-\kappa)-\Delta\phi_-(\eta+\tau-\kappa)]\hat{u} \\ &+[\Delta\phi_+(\eta-\tau+\kappa)-\Delta\phi_-(\eta+\tau+\kappa)]\hat{u}^*\} \end{aligned} \tag{8}$$

where: η is time normalized by the bit time, τ is normalized DGD, κ is normalized PSD and K is constant.

In this case, the direction of input SOP is aligned to the S_1 direction in Stokes space, which is the same as the PSP, and the direction of PSD depolarization is S_1-S_2, $\hat{u}$ and $\hat{u}^*$ represent left and right circular polarization respectively, the $\phi_\pm$ terms independent of κ are split pulses due to DGD, and the $\Delta\phi_\pm$ terms dependent on κ are additional split pulses due to PSD.

The PMDC operates to align the PSP to the input SOP, and the HOPC operates to align the polarization axis to the PSP, so only the x component is transmitted by the polarizer.

$$\begin{bmatrix} 1 & 0 \\ 0 & 0 \end{bmatrix} \cdot \hat{u}^{(*)} = (\hat{u}^*+\hat{u})/2 \tag{9}$$

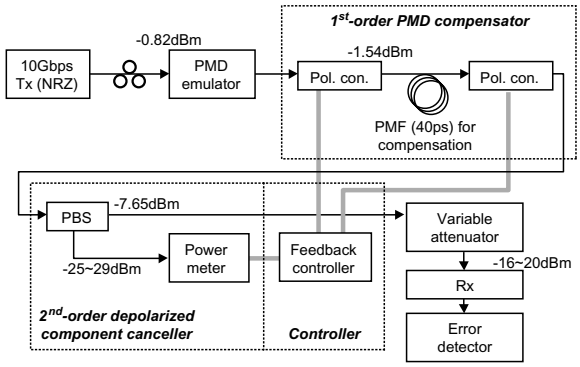

Figure 6 Configuration of NRZ test system.

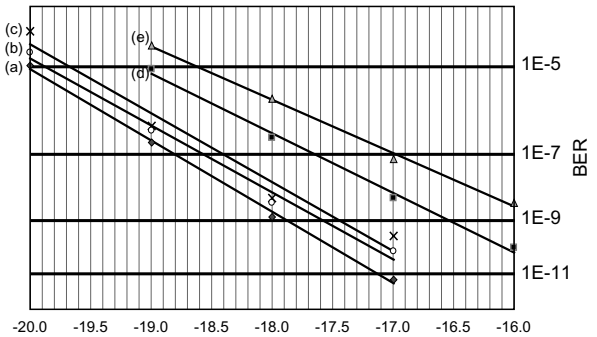

(a) Back to Back
(b) DGD 30 ps + SOPMD 441 ps^2 with our PMDC with HOPC (average with regard to the input SOP)
(c) DGD 30 ps + SOPMD 441 ps^2 with only 1st-order PMDC (average)
(d) DGD 30 ps (worst case),
(e) DGD 30 ps + SOPMD 441 ps^2 (worst case)

Figure 7 BER test results.

When the PMDC and HOPC are properly controlled, the transmitted pulse may be represented as

$$\mathrm{E}(\eta) = \frac{K}{\sqrt{2}}\{2\phi_+(\eta-\tau) + \frac{1}{2}[\Delta\phi_+(\eta-\tau-\kappa)+\Delta\phi_+(\eta-\tau+\kappa) - \Delta\phi_-(\eta+\tau-\kappa)-\Delta\phi_-(\eta+\tau+\kappa)]\}(\hat{u}^*+\hat{u}) \quad (10)$$

Since the $\Delta\phi_\pm$ terms dependent of κ are cut in half, the components of split pulses due to PSD are mitigated. The effect of PMDC with HOPC in mitigating second-order PMD is shown analytically.

4.3 Test Results

The 10-Gbps non-return zero (NRZ) test system that we used is shown in Figure 6. We configured the feedback loop using two polarization controllers, which are our proprietary magneto-optic polarization controller [12]. We used two states generated by the PMD emulator, namely 30-ps DGD without SOPMD and 30-ps DGD with 441 ps^2 SOPMD that consists of only a PSD component. Since the emulator we used here is made up of only two sections, SOPMD has only PSD components, and DGD and SOPMD have no frequency dependence.

Because our first-order PMDC operates so that the total PSP is identical to the input SOP to the system, the sum DGD of the transmission line and the PMF in the compensator varies in response to the connection angle between them. And second-order PMD is affected by DGD, so the penalty caused by second-order PMD varies depending on the input SOP. Therefore, we took the average BER with respect to input SOP when we used the PMDC with HOPC. In the case of no PMDC, we took the worst BER.

The BER test results are shown in Figure 7. The curves are (a) back to back, (b) DGD 30 ps + SOPMD 441 ps^2 with our PMDC with HOPC (average with regard to the input SOP), (c) DGD 30 ps + SOPMD 441 ps^2 with only first-order PMDC (average), (d) DGD 30 ps (worst case), (e) DGD 30 ps + SOPMD 441 ps^2 (worst case).

Curve (b) is the data for the novel configuration we propose and (c) is the data without PMDC. We can see that our simplified PMDC with HOPC can suppress the second-order PMD effect in the same way as the conventional configuration. The amount of suppression is not so dramatic (around 30% of the power penalty), but this method is very simple and inexpensive. It is necessary to check whether this device is adequate for use in actual transmission system or not.

5. CONCLUSION

We have proposed a PMD emulator on a variable Faraday rotator (VFR), and have confirmed that it is capable of generating a stable PMD spectrum. The two components of second-order PMD measured by the measurement system developed here agree with the theoretical calculations.

We also have proposed a novel simplified configuration consisting of a first-order PMDC with higher-order PMD canceller (HOPC). The operation of this device has been checked in a 10G-NRZ evaluation system, and it has been found that it can suppress the second-order PMD effect consisting of a PSD component.

It is certain that requirements in terms of transmission rates will increase as time goes on, and we cannot avoid the problems either of higher-order dispersion compensation or higher-order PMD compensation. A second-order PMD emulator will be useful for reaching a deeper understanding of second-order PMD effect and optimizing second-order compensators in their development.

REFERENCES

1) H. Ooi et al.: "Automatic polarization-mode dispersion compensation in 40-Gbit/s transmission", OFC'99, WE5-1 (1999), 86.
2) F. Bruyere: Optical Fiber Technol., 2 (1996), 269.
3) T. Takahashi et al.: "Automatic compensation technique for timewise fluctuation polarization mode dispersion in in-line amplifier systems", Electron. Lett., 30 (1994), 348.

4) F. Roy et al.: "A simple dynamic polarization mode dispersion compensator", OFC'99, TuS4-1 (1999), 275.
5) C. Francia et al.: Photon. Technol. Lett., 10 (1998), 1739.
6) F. Bruyere: IEEE Photon. Technol. Lett., 10 (1996), 696.
7) J. P. Gordon and H. Kogelnik: Proc. Nat. Acad. Sci., 97 (2000), 4541.
8) J. Poirrier et al.: OFC2002, W14 (2002), 236.
9) Mimura et al.: Proc. General Conference of IEICE 2003, B-10-119 (2003). (in Japanese)
10) R. M. Jopson, L. E. Nelson, and H. Kogelnik: IEEE Photon. Technol. Lett., 11 (1999), 1153.
11) K. Ikeda: OFC2003, MF90 (2003).
12) K. Ikeda: NFOEC2002, Technical Proceedings, (2002), 1965.